CNWRA *A center of excellence in earth sciences and engineering* ™

A Division of Southwest Research Institute®
6220 Culebra Road • San Antonio, Texas, U.S.A. 78228-5166
(210) 522-5160 • Fax (210) 522-5155

May 23, 2005
Contract No. NRC–02–02–012
Account No. 20.06002.01.322

U.S. Nuclear Regulatory Commission
ATTN: Mrs. Deborah A. DeMarco
Two White Flint North
11545 Rockville Pike
Mail Stop T8 A23
Washington, DC 20555

Subject: Programmatic review of paper for publication in the Preceedings of the Solid-Solid Phase Transformations in Inorganic Materials Conference on May 29–June 3, 2005

Dear Mrs. DeMarco:

Enclosed is the following paper with Form 390A being submitted for NRC programmatic review.

Modeling Phase Transformations of Ni-Cr-Mo Alloys
authored by Y.-M. Pan and D.S. Dunn

This paper summarizes the work conducted at the CNWRA on thermodynamic and kinetic modeling of phase transformations and solidification reactions in nickel-base alloys as influenced by alloy compositional variation. The work presented in this paper is largely drawn from the CNWRA 2004-01 report and the poster prepared for the subject conference that have been reviewed and approved by the NRC. The information on equilibrium phase diagram calculations for Alloy 686 weld filler metal presented in this paper has not been previously reviewed by the NRC.

Please advise me of the results of your programmatic review. If you have any questions regarding this poster, please contact Yi-Ming Pan at (210) 522-6640. Your cooperation in this matter is appreciated.

Sincerely,

for S. Mohanty

Sitakanta Mohanty
Assistant Director

AS:ln

Attachments

cc: W. Reamer, E. Whitt, B. Meehan, E. Collins, L. Kokajko, K. Stablein, J. Guttmann, A. Campbell, T. McCartin, T. Ahn, M. Bailey, A. Csontos, D. Brooks, T. Kobetz, B. Leslie, D. Galvin, W. Patrick, B. Sagar, Y.-M. Pan, G. Cragnolino, D. Dunn, L. Yang, O. Pensado, K. Chiang, L. Gutierrez (ltr only), P. Maldonado, Record Copy B, IQS, CNWRA EMs & Dirs. (ltr only)

Washington Office • Twinbrook Metro Plaza #210
12300 Twinbrook Parkway • Rockville, Maryland 20852-1606

Solid-Solid Phase Transformations in Inorganic Materials 2005 *Edited by J.M. Howe*
TMS (The Minerals, Metals & Materials Society), 2005

MODELING PHASE TRANSFORMATIONS OF Ni-Cr-Mo ALLOYS

Yi-Ming Pan and Darrell S. Dunn

Center for Nuclear Waste Regulatory Analyses, Southwest Research Institute
6220 Culebra Road; San Antonio, TX 78238-5166, USA

Keywords: Ni-Cr-Mo alloys, phase stability, thermodynamic calculations

Abstract

Ni-Cr-Mo alloys undergo phase transformations of topologically closed-packaged (TCP) phases when exposed to elevated temperatures that may impair their performance. The influence of alloy compositional variation on the stability of TCP phases and solidification reactions has been investigated in Ni-Cr-Mo alloys within the composition specifications for the base metal and element segregation in the weld. Thermodynamic calculations for both Alloy 22 (UNS N06022) base metal and Alloy 686 (UNS N06686) weld filler metal at the nominal compositions predicted that at 870 °C the P phase would be the only stable TCP phase. For Alloy 22, the calculated P-phase composition was consistent with the experimental values. Within the specified composition limits high Mo content was found to stabilize the P phase by increasing the P-phase solvus. Solidification simulations predicted the solidification paths as well as the critical temperatures for the bulk alloy composition as well as the dendrite core and interdendritic compositions in the weld. The calculated solidification path under moving boundary conditions was almost identical to that predicted by the Scheil-Gulliver simulation. A substantial increase in the P-phase solvus temperature was obtained in the interdendritic regions due to the segregation of Mo in the welded material. A solution-annealing temperature window between 1265 °C and 1325 °C was predicted.

Introduction

Modern Ni-Cr-Mo alloys with increasing resistance to corrosion and stress corrosion, such as Alloy 22 (UNS N06022) that is considered for high-level nuclear waste outer container application [1], have been developed by combining the benefits of Mo and Cr to prevent localized corrosion and reducing C content to avoid sensitization. However, these alloys undergo phase transformations when exposed to temperatures ranging from 600 to 900 °C that result in the formation of secondary topologically close-packed (TCP) phases, such as σ, P and μ [2-5]. Microstructural analyses revealed that precipitation of Mo-rich TCP phases in Alloy 22 base metal started at grain boundaries after thermal exposure [4,5]. Additionally, formation of a dendritic structure and the presence of element segregation with TCP phases in the interdendritic regions were evident in Alloy 22 weld metal [6-8]. The segregation of Mo in the solidified weld microstructure was found to promote the phase transformations of TCP phases. The preferential precipitation of TCP phases at grain boundaries and in interdendritic regions has been shown to decrease the localized corrosion resistance and impair the mechanical properties of thermally altered and welded Alloy 22 [7,9,10].

Elevated temperature exposure as a result of potential fabrication processes (i.e., welding and postweld treatments) may alter the microstructure and performance of the Alloy 22 waste package outer barrier. Solution annealing has been proposed by the U.S. Department of Energy [11] to

mitigate the detrimental effects of phase instability and remove residual stresses created by the forming and welding operations during the fabrication of the disposal containers. Solution annealing at 1125 °C as well as exposures to temperatures in the range of 600 to 900 °C were reported to enhance precipitation of the TCP phases in Alloy 22 welds, and thus, increase the susceptibility of Alloy 22 to localized corrosion [8,10]. Furthermore, the effect of compositional variations of the base alloy and weld filler metal on thermal stability and mechanical properties of Alloy 22 is a concern. It is necessary to understand the influence of fabrication processes and compositional variations on metallurgical stability and its effect on the corrosion and mechanical performance of both Alloy 22 base metal and welds. The objective of this study was to model the influence of alloy compositional variations on the stability of TCP phases and solidification reactions using Thermo-Calc Version N and DICTRA Version 21 (Diffusion Controlled TRAnsformation) computer codes. All of the calculations were compared to previously reported microstructural analysis of Alloy 22 materials [8].

Thermodynamic and Kinetic Calculations

In the thermodynamic and kinetic modeling, the thermodynamic properties for each phase are defined on the basis of the CALPHAD method (CALculation of PHAse Diagrams) [12]. The CALPHAD method employs a variety of mathematical models to describe the thermodynamic descriptions of the various phases. The thermodynamic data used by the models are held in the databases that can be accessed by Thermo-Calc and DICTRA to retrieve the thermodynamic and mobility data for performing simulations. Direct coupling of these two programs allows simulations of diffusion-controlled phase transformation processes.

For the Thermo-Calc calculations conducted in this study, input thermodynamic data to be used were retrieved from the Ni-DATA Version 5 database that was developed for multicomponent nickel-base alloys. The alloy compositions were input to the program. All equilibrium phase diagram calculations were run by conducting a single equilibrium calculation at a specific temperature, followed by a stepping calculation using temperature as an independent variable. Both equilibrium and Scheil-Gulliver solidification simulations were performed for the base alloy composition and the dendrite core and interdendritic compositions in the weld microstructures. All solidification simulations were initiated at a temperature above the liquidus and then stepped down with a 5 °C/s cooling step, typical of that anticipated for the solidification processes. The Scheil-Gulliver simulations assumed no back diffusion in solidified alloy whereas equilibrium was reached at each cooling step in the equilibrium simulations.

The kinetic solidification simulations were performed by coupling Thermo-Calc and DICTRA. Input thermodynamic and mobility data were retrieved from the Ni-DATA Version 5 database and the MOB2 database, respectively. The kinetic simulations applied a moving boundary diffusion model that has been developed and implemented into the DICTRA software. The general calculation scheme consists of two steps, diffusion and equilibrium. The diffusion step was assumed to take place in a matrix phase, and after each diffusion step there was a change in the average composition of the matrix. The new equilibrium corresponding to the new average composition can be calculated at each gridpoint during the equilibrium step using Thermo-Calc. The diffusion step was then repeated with the new composition profile in the matrix phase. Cooling rates of 1 and 10 °C/s were used in the kinetic simulations.

Results and Discussion

Equilibrium Diagram Calculations

Equilibrium phase diagrams calculated with Thermo-Calc and the Ni-Data Version 5 database are shown in Figure 1 for Alloy 22 base metal and Alloy 686 (UNS N06686) weld filler metal at their nominal compositions (in wt%) of Ni-21.25Cr-13.5Mo-3W-4Fe-0.01Co-0.03Si-0.004C and Ni-21Cr-16Mo-3.7W-4Fe-0.01Co-0.03Si-0.004C, respectively, as specified in ASTM B575 [13]. The two calculated phase fraction vs. temperature diagrams were similar, in which the P phase was the stable TCP phase at high temperatures, and the μ and γ′ phases coexisted with the P phase at lower temperatures. Note that in both Ni-Cr-Mo alloys the thermodynamic predictions for M_6C and $M_{23}C_6$ were not included in the equilibrium diagrams due to their low phase contents. The calculation for Alloy 22 predicted that the solidus and liquidus temperatures were 1353 °C and 1381 °C, respectively. The P-phase solvus temperature was predicted to be 1072 °C. The calculation also predicted that at 870 °C the P phase would be the only stable TCP phase. The calculated phase contents and compositions for the γ face-centered-cubic matrix, P, and M_6C phases at 870 °C are listed in Table I. The calculated P-phase composition was consistent with the experimental values measured by analytical electron microscopy [8]. Additionally, the phase fraction vs. temperature diagram for Alloy 686 in Figure 1 shows that the stability of the P phase was clearly enhanced by the high Mo content, as the P-phase solvus increased to 1218 °C.

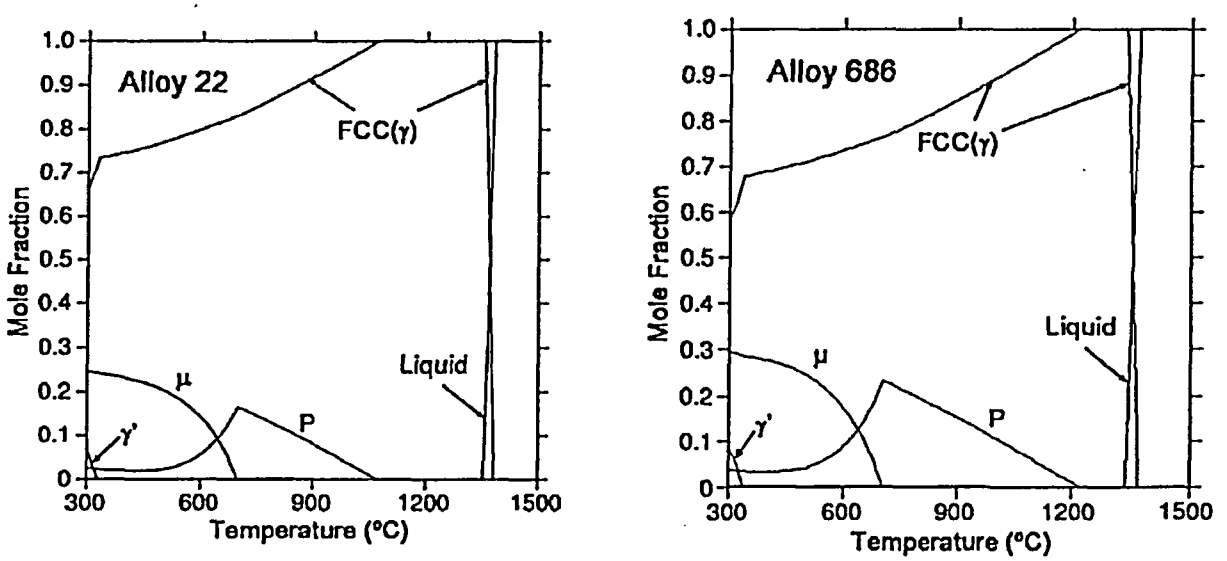

Figure 1: Calculated equilibrium phase fraction vs. temperature diagrams for Alloy 22 base metal and Alloy 686 weld filler metal

Table I. Calculated Phase Contents and Compositions in Alloy 22 at 870 °C

Phase	Amount		Chemical Content (wt%)							
	wt%	mole%	Ni	Cr	Mo	W	Fe	Co	Si	C
γ	88.43	90.48	62.13	21.55	10.07	1.78	4.42	0.011	0.034	0.001
P	11.46	9.42	28.28	18.99	39.56	12.39	0.78	0.005	—	—
M_6C	0.11	0.10	24.75	14.25	52.27	4.92	1.21	0.002	0.001	2.58

The predicted equilibrium TCP phases in Alloy 22 as a function of temperature differ from that reported by Turchi et al. using the SSOL database [14]. The σ phase was predicted to be stable from approximately 800 to 930 °C whereas the P phase was stable at temperatures below about 820 °C. Contrary to the predicted solvus temperature of 1072 °C for the P phase in the base metal, the maximum temperature for the σ phase predicted by Turchi et al. [14] was 930 °C. The observed discrepancy in the thermodynamic calculations could have been caused by the use of different databases.

The effect of compositional variation on the solvus temperature of P phase was evaluated by varying the composition between the specified limits for each element [13]. The baseline temperature was calculated based on the nominal alloy composition. The calculated P-phase solvus temperatures, as each element was changed between its maximum and minimum limits, are shown in Figure 2. The P-phase solvus temperature for the baseline composition was 1074 °C. Mo, as the major TCP phase forming element, exhibited the greatest sensitivity to the upper stability temperature of the P phase. With a maximum Mo content of 14.5 wt%, the calculated solvus temperature increased to 1121 °C. Other P-phase forming elements (i.e., Cr and W) also have a profound effect, whereas the influence of iron was attributed to the largest variation between its maximum and minimum limits (6.0 and 2.0 wt%). These results indicate that high Mo content stabilized the TCP phases and heat-to-heat compositional variations in the Alloy 22 base metal may influence the formation and dissolution of TCP phases.

Solidification Simulations

Solidification simulations were performed for Alloy 22 at the base alloy composition, as well as the experimentally determined compositions for the dendrite core and interdendritic regions of the deposited weld metal. The average compositions (in wt%) of the dendrite cores and the interdendritic regions measured by analytical electron microscopy were Ni-21.8Cr-13.0Mo-2.60W-2.75Fe and Ni-22.6Cr-18.0Mo-2.48W-2.48Fe, respectively [8]. Figure 3 shows the calculated

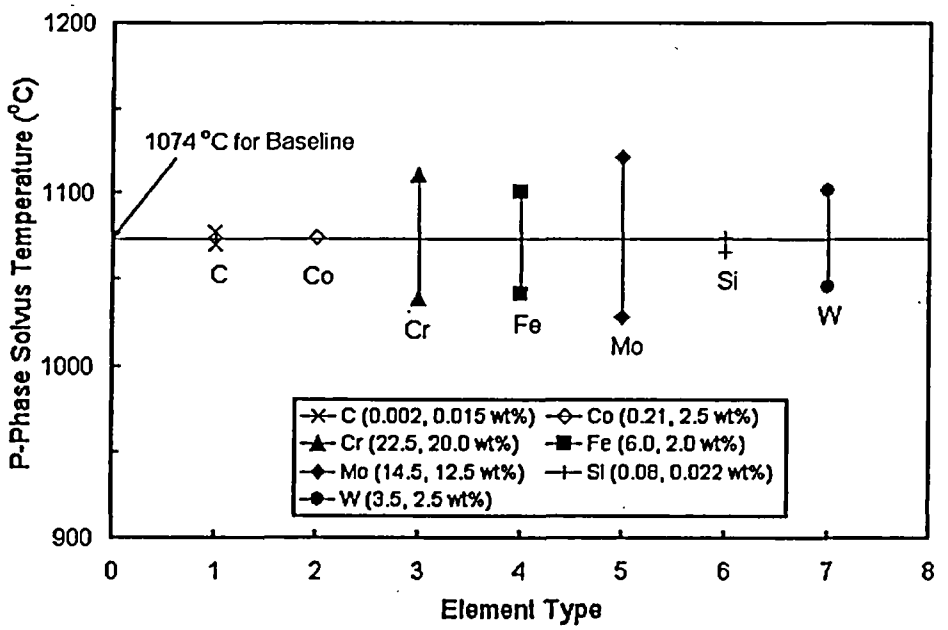

Figure 2: Variation in calculated P-phase solvus by varying each elements in Alloy 22 within its composition limits

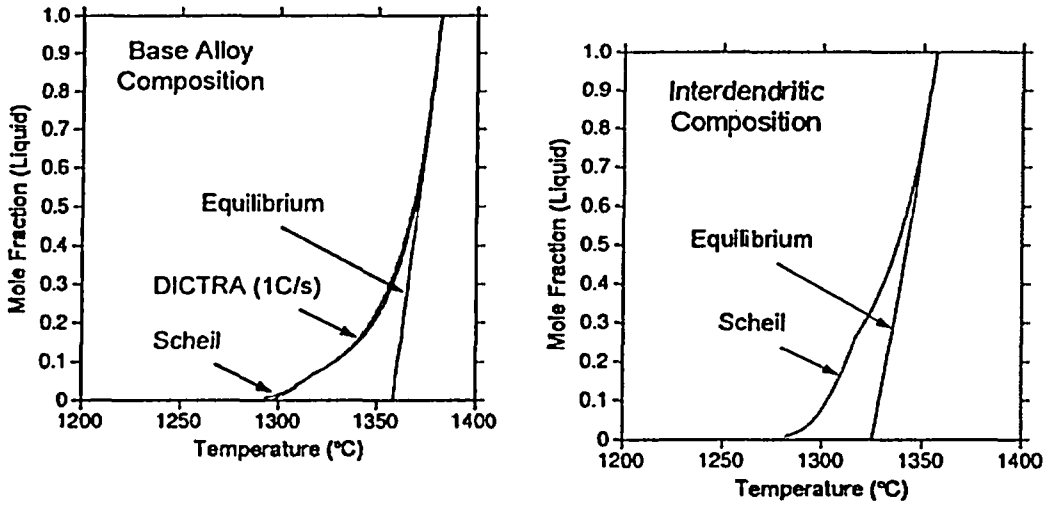

Figure 3: Solidification paths for Alloy 22 base metal composition and interdendritic composition in the weld microstructure

solidification paths for the base alloy composition and the interdendritic weld composition. In Thermo-Calc calculations, the equilibrium simulations predicted complete solidification of liquid to γ phase (face-centered cubic matrix) with P phase forming after solidification was complete whereas the Scheil-Gulliver simulations predicted the formation of P phase near the end of solidification. As also shown in Figure 3, the predicted solidification path for the base alloy composition from the Scheil-Gulliver simulation was almost identical to that from the kinetic DICTRA simulation with a cooling rate of 1 °C/s. A similar solidification path was also observed with a high cooling rate of 10 °C/s.

From these solidification simulations the predicted liquidus, solidus, and P-solvus temperatures are listed in Table II for both the equilibrium and Scheil-Gulliver simulations. In all cases, the Scheil-Gulliver simulations predicted a low solidus and a high P-phase solvus compared to the equilibrium simulations. For example, the Scheil-Gulliver simulation of the base alloy composition predicted a 65 °C decrease in solidus and a 252 °C increase in the P-phase solvus. Since equilibrium was reached in the solidified alloy at each cooling step, the equilibrium simulations predicted an accurate solidus temperature. Thus, the calculated lowest solidus temperature of 1325 °C in the interdendritic region can be used as an upper temperature bound. The equilibrium simulations also predicted a high solvus temperature of 1265 °C for the P-phase in the interdendritic region due to Mo segregation, which can be used as a lower temperature bound for dissolving the secondary precipitates. The solidification simulation results suggested a solution-annealing temperature

Table II. Calculated Liquidus, Solidus, and P-Phase Solvus in Alloy 22 (°C)

Location	Equilibrium Simulation			Scheil-Gulliver Simulation		
	Liquidus	Solidus	P-Solvus	Liquidus	Solidus	P-Solvus
Dendrite Core	1382	1358	1018	1382	1292	1310
Interdendritic Region	1357	1325	1265	1357	1287	1316
Base Alloy	1380	1356	1062	1380	1291	1314

window in the range of 1265 and 1325 °C, significantly higher than the currently proposed solution-annealing treatment of the Alloy 22 outer cylinders at 1150 °C [11]. It should be noted that the chemical compositions of the base alloy and weld filler metal, as well as the solidification conditions, would be expected to affect the degree of segregation, and thus, the phase transformation temperatures. Since high Mo content was observed to stabilize the P phase, the minimum solution-annealing temperature is expected to increase with increasing Mo content in the solidified weld microstructure. Additional evaluation may be necessary in assessing the solution-annealing treatment and the possible detrimental effects of fabrication processes on the localized corrosion and mechanical performance of the Alloy 22 waste package outer containers.

Conclusions

Phase transformations of Ni-Cr-Mo Alloys were modeled in the present study and the conclusions are summarized as follows:

1. Thermodynamic calculation for Alloy 22 predicted the formation of P phase at 870 °C. The calculated P-phase composition was consistent with the experimental measurements.
2. The calculated P-phase solvus temperatures within the possible composition variations for Alloy 22 base metal indicate that Mo had the most profound effect on the formation and dissolution of TCP phases.
3. Solidification simulations predicted a high P-phase solvus in the interdendritic regions of the deposited weld metal. The high stability temperature of the P phase was attributed to the Mo segregation in the weldments.
4. Critical temperatures predicted by solidification simulations suggested a solution-annealing temperature window in the range of 1265 and 1325 °C for the Alloy 22 weld metal studied in this investigation.

Acknowledgments

This paper was prepared to document work performed by the Center for Nuclear Waste Regulatory Analyses (CNWRA) and its contractors for the Nuclear Regulatory Commission (NRC) under Contract No. NRC–02–02–012. The activities reported here were performed on behalf of the NRC Office of Nuclear Material Safety and Safeguards, Division of High-Level Waste Repository Safety. This paper is an independent product of the CNWRA and does not necessarily reflect the view or regulatory position of the NRC.

References

1. "Technical Basis Document No. 6: Waste Package and Drip Shield Corrosion," Revision 1, DOE Yucca Mountain Project, Las Vegas, NV: Bechtel SAIC Co., 2003.
2. M. Raghavan, R.R. Mueller, G.A. Vaughn, and S. Floreen: *Metall. Trans.*, 1984, vol. 15A, pp. 783–792.
3. E. Gozlan, M. Bamberger, S.F. Dirnfeld, B. Prinz, and J. Klodt: *Mater. Sci. Eng.*, 1991, vol. 141A, pp. 85–95.
4. T.S.E. Summers, M.A. Wall, M. Kumar, S.J. Matthews, and R.B. Rebak: Scientific Basis for Nuclear Waste Management XII, Symposium Proc. vol. 556, Materials Research Society, Warrendale, PA, 1999, pp. 919–926.
5. Y.-M. Pan, D.S. Dunn, and G. Cragnolino: *Electron Microscopy—Its Role in Materials Science: the Mike Meshii Symposium*, The Minerals, Metals, and Materials Society, Warrendale, PA, 2003, pp. 201–208.

6. M.J. Cieslak, T.J. Headley, and A.D. Romig, Jr.: *Metall. Trans.*, 1986, vol. 17A, pp. 2035–2047.
7. T.S.E. Summers, R.B. Rebak, T.A. Palmer, and P. Crook: Scientific Basis for Nuclear Waste Management XXV, Symposium Proc. vol. 713, Materials Research Society, Warrendale, PA, 2002, pp. 45–52.
8. Y.-M. Pan, D.S. Dunn, and G.A. Cragnolino: *Metall. Mater. Trans.*, 2005, vol. 36A, pp. 1143–1151.
9. U.L. Heubner, E. Altpeter, M.B. Rockel, and E. Wallis, *Corrosion*, 1989, vol. 45, pp. 249–259.
10. D.S. Dunn, Y.-M. Pan, K.T. Chiang, L. Yang, G.A. Cragnolino, and X. He: *J. of Metals*, Jan. 2005, pp. 49–55.
11. "Waste Package Operations Fabrication Process Report," DOE Yucca Mountain Project, TDR-EBS-ND-000003, Rev. 02, Las Vegas, NV: Bechtel SAIC Co., 2001.
12. N. Saunders and A.P. Miodownik: "CALPHAD (Calculation of Phase Diagrams): A Comprehensive Guide," Pergamon Materials Series. vol. 1. R.W. Cahn, ed. New York City, NY: Elsevier Science, 1998.
13. *ASTM Annual Book of Standards*, ASTM Standard B575-04, ASTM, Philadelphia, PA, 2004, vol. 02.04.
14. P.E.A. Turchi, L. Kaufman, and Z-K. Liu: Scientific Basis for Nuclear Waste Management XXVI, Symposium Proc. vol. 757, Materials Research Society, Warrendale, PA, 2003, pp. 729–734.